AMERICAN SOCIETY FOR MICROBIOLOGY | Journal of Bacteriology

$F_{420}H_2$ Is Required for Phthiocerol Dimycocerosate Synthesis in Mycobacteria

Endang Purwantini,[a] Lacy Daniels,[c] Biswarup Mukhopadhyay[a,b]

Department of Biochemistry[a] and Virginia Bioinformatics Institute,[b] Virginia Tech, Blacksburg, Virginia, USA; Department of Pharmaceutical Sciences, Irma Lerma Rangel College of Pharmacy, Texas A&M Health Science Center, Kingsville, Texas, USA[c]

ABSTRACT

Phthiocerol dimycocerosates (PDIM) are a group of cell surface-associated apolar lipids of *Mycobacterium tuberculosis* and closely related mycobacteria, such as *Mycobacterium bovis* and *Mycobacterium leprae*. A characteristic methoxy group of these lipids is generated from the methylation of a hydroxyl group of the direct precursors, the phthiotriols. The precursors arise from the reduction of phthiodiolones, the keto intermediates, by a ketoreductase. The putative phthiodiolone ketoreductase (PKR) is encoded by Rv2951c in *M. tuberculosis* and BCG_2972c in *M. bovis* BCG, and these open reading frames (ORFs) encode identical amino acid sequences. We investigated the cofactor requirement of the BCG_2972c protein. A comparative analysis based on the crystallographic structures of similar enzymes identified structural elements for binding of coenzyme F_{420} and hydrophobic phthiodiolones in PKR. Coenzyme F_{420} is a deazaflavin coenzyme that serves several key functions in pathogenic and nonpathogenic mycobacteria. We found that an *M. bovis* BCG mutant lacking F_{420}-dependent glucose-6-phosphate dehydrogenase (Fgd), which generates $F_{420}H_2$ (glucose-6-phosphate + $F_{420} \rightarrow$ 6-phosphogluconate + $F_{420}H_2$), was devoid of phthiocerols and accumulated phthiodiolones. When the mutant was provided with $F_{420}H_2$, a broken-cell slurry of the mutant converted accumulated phthiodiolones to phthiocerols; $F_{420}H_2$ was generated *in situ* from F_{420} and glucose-6-phosphate by the action of Fgd. Thus, the reaction mixture was competent in reducing phthiodiolones to phthiotriols (phthiodiolones + $F_{420}H_2 \rightarrow$ phthiotriols + F_{420}), which were then methylated to phthiocerols. These results established the mycobacterial phthiodiolone ketoreductase as an $F_{420}H_2$-dependent enzyme (fPKR). A phylogenetic analysis of close homologs of fPKR revealed potential F_{420}-dependent lipid-modifying enzymes in a broad range of mycobacteria.

IMPORTANCE

***Mycobacterium tuberculosis* is the causative agent of tuberculosis, and phthiocerol dimycocerosates (PDIM) protect this pathogen from the early innate immune response of an infected host. Thus, the PDIM synthesis system is a potential target for the development of effective treatments for tuberculosis. The current study shows that a PDIM synthesis enzyme is dependent on the coenzyme F_{420}. F_{420} is universally present in mycobacteria and absent in humans. This finding expands the number of experimentally validated F_{420}-dependent enzymes in *M. tuberculosis* to six, each of which helps the pathogen to evade killing by the host immune system, and one of which activates an antituberculosis drug, PA-824. This work also has relevance to leprosy, since similar waxy lipids are found in *Mycobacterium leprae*.**

Diacylated polyketides (DPs), a family of waxy compounds, are found in the cell walls of a group of mostly pathogenic and slow-growing mycobacteria (Fig. 1) (1, 2). The pathways for the biosynthesis of DPs are of great interest because these compounds are virulence factors for *Mycobacterium tuberculosis* and *Mycobacterium leprae*, which cause tuberculosis (TB) and leprosy, respectively (3–11). It was recently shown that these polyketide derivatives protect *M. tuberculosis* from the early innate immune response of an infected host (12). The DPs are generated by esterifying β-glycol-containing long-chain polyketides (PK) with long-chain multimethyl-branched fatty acids (Fig. 1) (1, 2). In *M. tuberculosis*, these compounds have two structural types: phthiocerol dimycocerosates (PDIM or DIM A) and glycosylated phenolphthiocerol dimycocerosates or phenolic glycolipids (PGL-tb) (13) (Fig. 1); if the PK units carry a keto group in place of a methoxy group, the respective variations are called phthiodiolone dimycocerosates (DIM B) and glycosylated phenolphthiodiolone dimycocerosates (Fig. 1) (13–15). The above-mentioned methoxy group is generated in two steps, i.e., reduction of the corresponding keto group to a hydroxy group by a phthiodiolone reductase, generating phthiotriol intermediates, followed by methylation of the hydroxy group by a methyltransferase (14, 15).

In *Mycobacterium tuberculosis*, the open reading frames (ORFs) Rv2951c and Rv2952 encode the phthiodiolone ketoreductase (PKR) and phthiotriol methyltransferase, respectively (13–15). Disruption of Rv2951c eliminates the production of DIM A and PGL-tb and causes the accumulation of DIM B and glycosylated phenolphthiodiolone dimycocerosates (13). It has been indicated that Rv2951c encodes a domain characteristic of coenzyme F_{420}-dependent N^5,N^{10}-methylene tetrahydrometha-

Received 23 December 2015 **Accepted** 6 May 2016

Accepted manuscript posted online 16 May 2016

Citation Purwantini E, Daniels L, Mukhopadhyay B. 2016. $F_{420}H_2$ is required for phthiocerol dimycocerosate synthesis in mycobacteria. J Bacteriol 198:2020–2028. doi:10.1128/JB.01035-15.

Editor: T. M. Henkin, Ohio State University

Address correspondence to Endang Purwantini, epurwant@vt.edu.

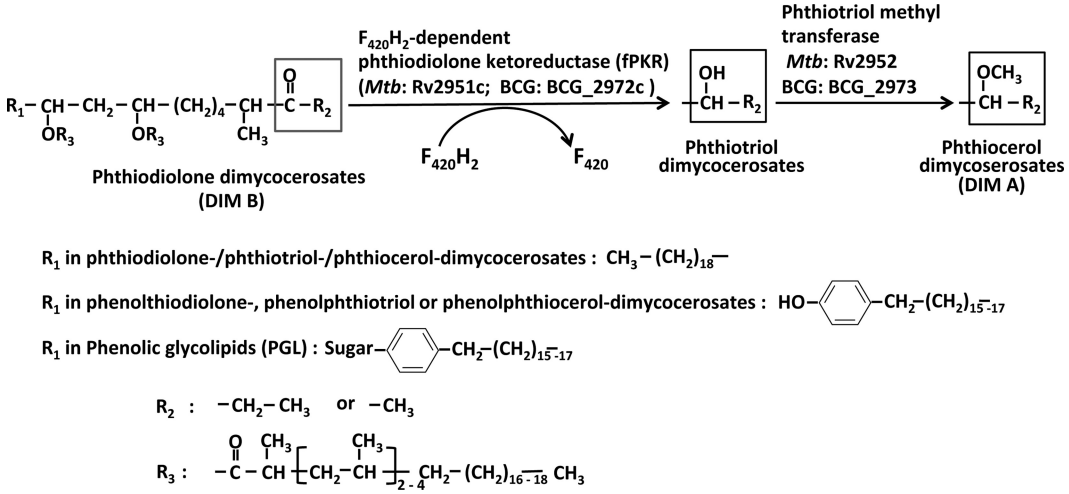

FIG 1 Conversion of phthiodiolone dimycocerosates (DIM B) to phthiocerol dimycocerosates (DIM A) in mycobacteria. The conversion proceeds via intermediate formation of phthiotriol dimycocerosates by an $F_{420}H_2$-dependent phthiodiolone ketoreductase (fPKR) that is encoded by Rv2951c in *Mycobacterium tuberculosis* (*Mtb*) and by BCG_2972c in *Mycobacterium bovis* BCG. The structures of the three classes of dimycocerosates are shown.

nopterin reductase (Mer), but its specific cofactor requirement has not been determined (14). Mer is a key enzyme in methane biosynthesis in methanogenic archaea (16), and a well-characterized mycobacterial Mer homolog is F_{420}-dependent glucose-6-phosphate (G6P) dehydrogenase (Fgd) (17–19); all mycobacteria carry the *fgd* gene (19, 20).

Coenzyme F_{420}, a deazaflavin derivative, is a major coenzyme of the methanogenic archaea and of methanogens (16). In the bacterial domain, it is mostly found in some of the actinobacterial species, including all mycobacteria and streptomyces, and genome analysis suggests that F_{420} is sporadically present in proteobacteria as well (20–23). At the ground state, the most commonly encountered form of this coenzyme in biological systems, the midpoint redox potential value (E_0') of F_{420} is −360 mV, and it performs hydride transfer (16, 24). The E_0' value of $NAD(P)^+$, a major biological hydride transfer coenzyme, is −320 mV (16, 24). Whether the actinobacteria benefit from the higher reducing power (lower E_0' value) of F_{420} remains to be determined.

In this report, we describe results from our genetic and chemical analyses and an *in vitro* enzymatic conversion experiment which show that PKR is indeed an F_{420}-dependent enzyme, and accordingly, we have termed it fPKR.

MATERIALS AND METHODS

Growth medium and culture conditions for *Mycobacterium bovis* BCG. *M. bovis* BCG strain Pasteur 1173P2 (wild type) and a respective mutant strain lacking functional *fgd* (ORF BCG_0446) (25, 26) were used in this study. The mutant strain was obtained during a previous Tn*5367* mutagenesis-based study, and it is known to lack the respective enzymatic activity (26). To clearly map the Tn*5367* insertion site in the *M. bovis* BCG *fgd*::Tn*5367* strain, a region of the mutant chromosome containing the interrupted *fgd* gene, respective upstream and downstream regions, and the inserted transposon was amplified by use of primers BCGFgd/1F (5′ GGATCCGTCGCCGGGATAGCCGGCGTC3′) and BCGFgd/2R (5′ CTGCAGGTCCCGCTCCGCAGAGAGCCG3′), and the amplicon was sequenced. The data showed that the transposon was inserted at the 421-bp position of the *fgd* coding sequence.

Both the wild-type and *fgd*::Tn*5367* strains were grown in Middlebrook 7H9 liquid medium supplemented with 5% Middlebrook ADC, 0.2% glycerol, and 0.05% Tween 80 (27); the *fgd*::Tn*5367* strain was cultivated in the presence of kanamycin (20 μg/ml). The cultures were incubated at 37°C with occasional manual shaking for 2 to 3 weeks. The cells were recovered by centrifugation at 18,000 × *g* for 15 min at 4°C, washed with 20 mM potassium phosphate buffer, pH 7.0, and stored at −20°C until further use.

Heterologous expression and purification of F_{420}-dependent glucose-6-phosphate dehydrogenase. The coding sequence of *Mycobacterium smegmatis fgd* (*msmeg_0777*) (19) was PCR amplified and cloned into the NdeI and BamHI sites of pTEV5, a T7 promoter-based protein expression vector (28), providing pTEV5-*msmeg_0777*. The plasmid was designed to generate recombinant Fgd with an NH_2-terminal His_6 tag (MSYYHHHHHHDYDIPTSENLYFQGASH). *Escherichia coli* BL21(DE3)(pTEV5-*msmeg_0777*) was cultivated at 37°C in LB medium containing 100 μg/ml ampicillin. Fgd expression was induced by supplementing the culture with isopropyl-β-D-thiogalactopyranoside (IPTG) to a final concentration of 0.4 mM. Fgd carrying the His_6 tag was purified as a soluble protein via Ni^{2+}-nitrilotriacetic acid chromatography (29, 30); the enzyme was eluted with 150 mM imidazole, and based on the results of SDS-PAGE analysis, the preparation was judged to be apparently homogeneous. Freshly prepared enzyme was used in the *in vitro* conversion experiment.

***In vitro* conversion of phthiodiolones to phthiotriols.** A broken-cell slurry of *M. bovis* BCG *fgd*::Tn*5367* was prepared as described previously (26). In brief, about 0.2 g of wet cells was resuspended in 0.2 ml 20 mM potassium phosphate buffer, pH 7, and the cells in this suspension were lysed by use of a mini-bead beater (BioSpec Products, Inc., Bartlesville, OK) operating at 4,800 rpm; three 1-min bead beatings with intermediate 2-min incubations on ice were used. The cell slurry (0.25 ml) was mixed with the following at the indicated final concentrations in a total volume of 0.5 ml: purified recombinant Fgd (20 μg), F_{420} (50 μM), and glucose-6-phosphate (5 mM). The mixture was incubated overnight at 37°C with gentle shaking. The apolar lipids were isolated from the mixture and analyzed via thin-layer chromatography (TLC) as described below.

Lipid analysis. A cell pellet (about 1 g) of *M. bovis* BCG or its *fgd*::Tn*5367* derivative was mixed with 20 ml of a mixture of chloroform-methanol (2:1 [vol/vol]) and shaken at room temperature (~25°C) overnight. The mixture was filtered using a Whatman grade 1 filter paper (GE Healthcare Bio-Sciences, Pittsburgh, PA), and then a 0.3% aqueous NaCl solution (1/5 of the filtrate volume) was added to the resulting filtrate to generate a chloroform layer that contained the apolar lipids, including DIM A and DIM B. The chloroform layer was collected and dried under an N_2 stream, and the residue was dissolved in a minimal volume of a

chloroform-methanol mixture (2:1 [vol/vol]). This product was analyzed via TLC on an aluminum-backed silica gel plate (Merck 5735, silica gel 60F254; Merck KGaA, Darmstadt, Germany), using a mixture of petroleum ether and diethyl ether (9:1) as the development solvent (15). The lipid spots of resolved lipids were visualized by spraying with a 5% molybdophosphoric acid solution in ethanol followed by charring at 110°C for 15 min (15); this procedure detects DIM A and DIM B but not the respective phenolic glycolipids (Fig. 1).

Mass spectrometric analysis of DIM A and DIM B. The lipids to be analyzed were purified via TLC as follows. To generate an adequate amount of material, the TLC analysis as shown in each lane of Fig. 3 was scaled to a multilane format, and a terminal lane was cut off and processed for the detection of DIM A and/or DIM B bands as described above. Using a relevant band in the terminal lane as a guide, the silica layers of the desired dimycocerosate spots were scraped from the rest of the lanes. From the recovered silica particles, dimycocerosates were extracted with chloroform-methanol (2:1) and analyzed via matrix-assisted laser desorption ionization–time of flight (MALDI-TOF) mass spectrometry at the School of Chemical Sciences Mass Spectrometry Laboratory at the University of Illinois at Urbana-Champaign. Bruker peptide calibration mixture II (angiotensin II, angiotensin I, substance P, bombesin, ACTH clip 1–17, ACTH clip 18–39, somatostatin 28, bradykinin fragment 1–7, and porcine renin substrate tetradecapeptide; covered mass range, ~700 to 3,200 Da) was used for calibration, and the matrix was 2,5-dihydroxybenzoic acid. A Bruker UltrafleXtreme mass spectrometer (Bruker, Bremen, Germany) equipped with a Smart Beam II laser was used in the positive mode to acquire MALDI-TOF mass spectra. Samples were analyzed in the reflectron mode.

Bioinformatic analysis. Homologs of the Rv2951c protein were identified via a BLASTP search (31) of the NCBI's nonredundant protein database, using the amino acid sequence of this protein as the query and with a specific focus on *Mycobacterium* species (taxid 1763). Proteins showing >50% identity to the Rv2951c protein were selected for a phylogenetic analysis, which was performed as described previously (32). In brief, the amino acid sequences were aligned and trimmed by use of the Muscle (33) and Gblocks (34) programs, respectively. A phylogenetic tree was then constructed using a maximum likelihood-based phylogenetic reconstruction program, proml, in the Phylip 3.67 package (32), with 100 replicates, and the tree was viewed with FigTree v1.4.2 (http://tree.bio.ed.ac.uk/software/figtree/).

For identification of the conserved Mer-type secondary structure features and F_{420}-binding residues and for prediction of the DIM B-interacting elements in the Rv2951c protein, the amino acid sequences of this protein and selected Mer homologs for which X-ray crystallographic three-dimensional structures of the F_{420}-bound forms are available (17, 35–37) were aligned by PROMALS3D at http://prodata.swmed.edu/promals3d/promals3d.php and by manual adjustments (38).

RESULTS AND DISCUSSION

Analysis of the structural characteristics of the Rv2951c protein. The goal of this analysis was to determine whether the Rv2951c protein has the potential to interact with coenzyme F_{420} and hydrophobic substrates, such as phthiodiolones. For this purpose, we performed a structure-based sequence alignment (Fig. 2) by utilizing the X-ray crystallographic structures of Mer from two methanogenic archaea, *Methanopyrus kandleri* and *Methanosarcina barkeri* (MkMer and MbMer, respectively) (36, 37), and two Mer homologs, an F_{420}-dependent secondary alcohol dehydrogenase (Adf) from another methanogen (35) and Fgd of *M. tuberculosis* (17) (Fig. 2). For Fgd, Adf, and MbMer, structures of F_{420}-bound forms were used. The primary structure of the recently described F_{420}-dependent hydroxymycolic acid dehydrogenase of *M. tuberculosis* (fHMAD or Rv0132c) (39) was also included in the analysis (Fig. 2). The alignment showed that the predicted secondary structural features of the Rv2951c protein are highly similar to those found in Fgd, Adf, and MbMer and that the protein carries the features that allow a Mer homolog to bind F_{420} (Fig. 2). Mer, Adf, and Fgd induce a butterfly conformation at the *si* face of bound F_{420} by holding the coenzyme with conserved structural elements (marked with asterisks in Fig. 2) (17, 35–37). In Adf, His^{39} and Glu^{108} hold the pyrimidine ring of F_{420}, and the hydroxybenzyl wing of the coenzyme is fixed by Val^{193} and Ile^{227} (35). These interactions are conserved in Fgd and Mer, the equivalent residues in fHMAD are His^{78} and Glu^{147}, and those in the Rv2951c protein are His^{43} and Glu^{129} (Fig. 2). In Adf, Fgd, and Mer, the central pyridine ring of F_{420} is placed outside the plane of the two flanking rings via an unusual structural element, a bulge, that contains a nonprolyl *cis*-peptide bond (17, 35–37). Among Mer homologs, this element was first identified in MkMer, where Gly^{64} and Ile^{65} form the unusual *cis*-peptide bond (37) (Fig. 2). In Fgd, this bond occurs between Ser^{73} and Val^{74}, and the carbonyl oxygen of Ser^{73} and the side chain of Val^{74} interact with the *re* face of the central pyridine ring (17). The respective residues in other enzymes are as follows (Fig. 2): Cys^{72} and Ile^{73} in Adf, Gly^{61} and Val^{62} in MbMer, Gly^{64} and Ile^{65} in MkMer, Gly^{121} and Val^{122} in fHMAD, and Cys^{94} and Val^{95} in the Rv2951c protein. The replacement of Ser^{73} as in Fgd with Cys or Gly in other Mer homologs is considered conservative, as these three amino acids are highly compatible in terms of their hydrophobicities, isoelectric points, and volumes (39–43). In Adf, the formation of the unfavorable nonprolyl *cis*-peptide bond is dictated by a highly conserved Asp residue (Asp^{38}) (Fig. 2), and the position of the carboxylate of this residue is fixed by a salt bridge with an Arg residue (Arg^{79}) (35). Both Asp^{38} and Arg^{79} of Adf are conserved in Fgd, MkMer, MbMer, fHMAD, and the Rv2951c protein (Fig. 2), and the previously reported consensus sequence for the bulge [D/E-H-$X_{(20–30)}$-I/L-S/G-X-I/V/A-X_5-R/H] (35) fits the Rv2951c protein. Thus, the Rv2951c protein carries all sequence features for binding coenzyme F_{420}.

In Adf, the hydroxybenzyl unit of F_{420} interacts with Val^{193} and Leu^{227}, which are hydrophobic, and this selection is justified by the localization of the hydrocarbon chain of the secondary alcohol in this region (35). Similarly, for MkMer, the equivalent region carries Ala^{197} and Tyr^{229}, which are proposed to interact with the pterin ring of tetrahydromethanopterin (37). A partial conservation is seen in fHMAD (Ala^{232} and Glu^{263}), which also oxidizes hydrophobic substrates, i.e., hydroxymycolic acids (39). In contrast, the homologous residues in Fgd are Ser^{196} and Glu^{230}, the latter of which is followed by Lys^{232}, and these elements not only accommodate the hydroxybenzyl ring but also will be near the charged glucose-6-phosphate (17). Based on these observations, the presence of Val^{215} and Val^{248} at the equivalent positions and an absence of the conservation of Lys^{232} of Fgd in the Rv2951c protein are consistent with the possibility that the Rv2951c protein acts on DIM B, a rather hydrophobic substrate. Hence, the Rv2951c protein has the structural elements for binding both F_{420} and the hydrophobic phthiodiolone moiety of DIM B and glycosylated phenolphthiodiolone dimycocerosates. These observations support the hypothesis that the Rv2951c protein utilizes $F_{420}H_2$ as the electron source for the reduction of phthiodiolone.

Genetic analysis of the requirement for $F_{420}H_2$ in phthiodiolone reduction. Our strategy for testing the above-mentioned hypothesis was based on the following observations. Several studies have shown that, at least under laboratory growth conditions

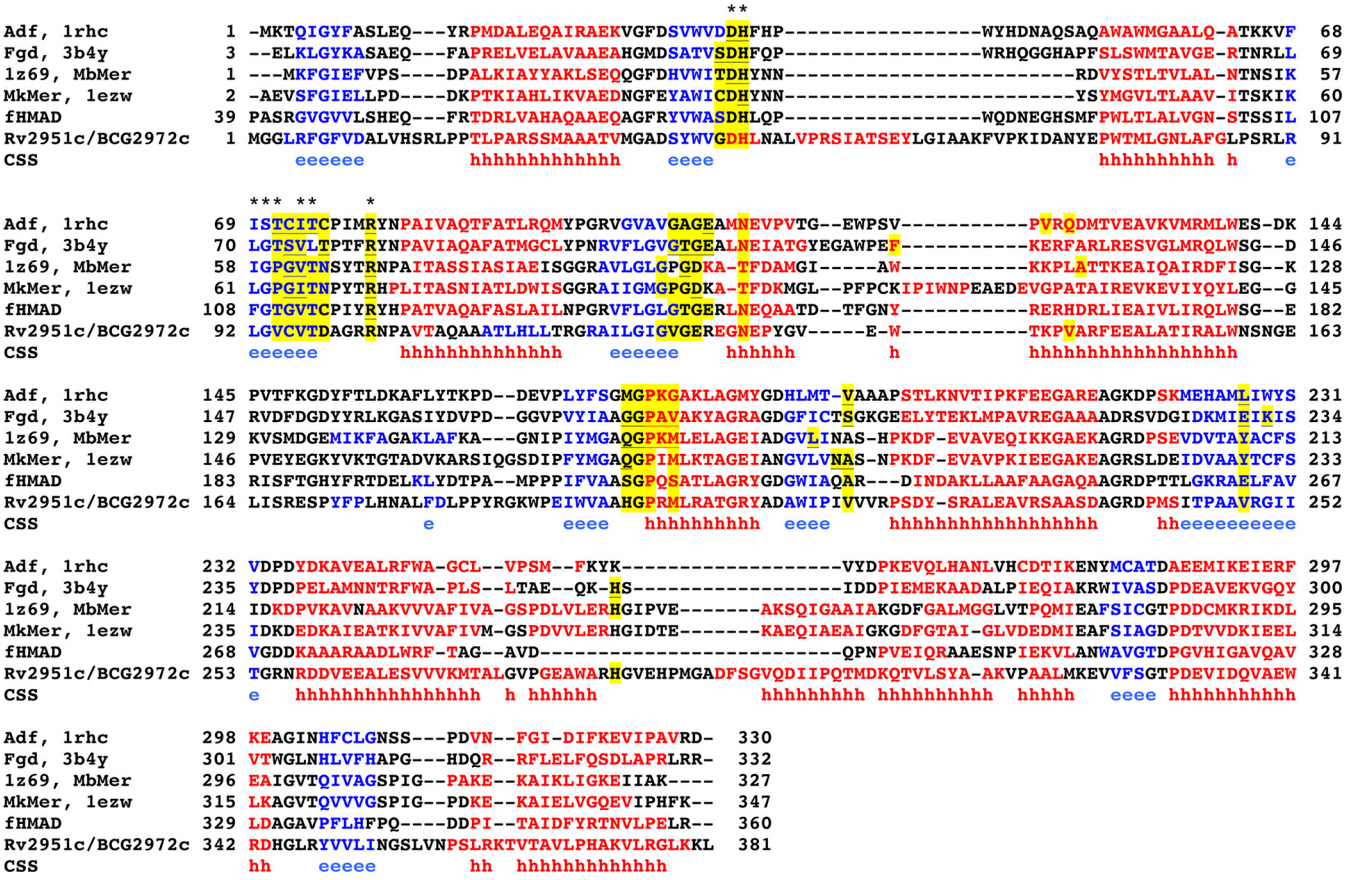

FIG 2 Putative F_{420}-binding residues in F_{420}-dependent phthiodiolone ketoreductase (fPKR). The figure presents a structure-guided multiple-sequence alignment generated at the PROMALS3D Web server (38). The ORFs encoding fPKR in *Mycobacterium tuberculosis* H37Rv (Rv2951c; http://www.ncbi.nlm.nih.gov/protein/CCP45755.1) and *Mycobacterium bovis* BCG strain Pasteur 1173P2 (BCG_2972c; http://www.ncbi.nlm.nih.gov/protein/CAL72961.1) have identical sequences. The sequences aligned (full name, abbreviation, PDB ID wherever applicable) are as follows: F_{420}-dependent secondary alcohol dehydrogenase from *Methanoculleus thermophilicus*, Adf, 1rhc (35); F_{420}-dependent glucose-6-phosphate dehydrogenase of *M. tuberculosis*, Fgd, 3b4y (17); F_{420}-dependent methylenetetrahydromethanopterin reductase of *Methanosarcina barkeri*, MbMer, 1z69 (36, 37); F_{420}-dependent methylenetetrahydromethanopterin reductase of *Methanopyrus kandleri*, MkMer, 1ezw (36, 37); F_{420}-dependent hydroxymycolic acid dehydrogenase of *M. tuberculosis*, fHMAD (http://www.ncbi.nlm.nih.gov/protein/P96809.1) (39); and F_{420}-dependent phthiodiolone ketoreductase, Rv2951c/BCG_2972c (this report). Yellow-shaded, underlined residues, experimentally determined F_{420}-binding residues (17, 35, 36); yellow-shaded residues, predicted F_{420}-binding residues; amino acid residues in red and blue letters, known (Adf, Fgd, MbMer, and MkMer) and predicted (fHMAD and fPKR) locations of alpha helices and beta sheets, respectively; CSS, consensus secondary structure (red h's and blue e's represent alpha helices and beta sheets, respectively); *, residues responsible for inducing a butterfly conformation at the *si* face of bound F_{420} (17, 35–37).

where glycerol or glucose is used as the carbon and energy source, Fgd is the major $F_{420}H_2$-generating enzyme in the mycobacteria, and elimination or disruption of the *fgd* gene blocks $F_{420}H_2$-dependent reactions. For example, the *M. smegmatis* Δ*fgd* strain cannot carry out reduction of NO_2, which requires $F_{420}H_2$ (44). Similarly, in *M. tuberculosis* and *M. bovis* BCG, inactivation of the *fgd* gene makes these organisms resistant to PA-824 (45); PA-824 as such is not an antimycobacterial agent, but its reaction with $F_{420}H_2$ as catalyzed by a deazaflavin-dependent nitroreductase (Ddn) releases NO that helps to kill mycobacteria (46, 47). Also, inactivation of the *fgd* gene eliminates aflatoxin degradation capability in *M. smegmatis*, as this process requires the actions of two families of $F_{420}H_2$-dependent reductases (48). A study with a mutant lacking Fgd activity helped to establish the role of $F_{420}H_2$ in the defense against oxidative stress in mycobacteria (49). Accordingly, we rationalized that if the Rv2951c protein uses $F_{420}H_2$ as the electron source for reducing phthiodiolone, an *M. tuberculosis* strain lacking functional *fgd* will produce DIM B and glycosylated phenolphthiodiolone dimycocerosates but not the respective phthiotriol forms, and therefore will lack DIM A and PGL-tb (Fig. 1).

We tested the above-mentioned hypothesis in the *Mycobacterium bovis* BCG model by using genetic analysis. The DIM A and DIM B profiles of this organism and *M. tuberculosis* are the same (14, 15, 50, 51). The homolog of the Rv2951c protein of *M. tuberculosis* in *M. bovis* BCG is the BCG_2972c protein, and these proteins have identical amino acid sequences (25). *M. bovis* BCG produces DIM A and DIM B (Fig. 3, wt lane) and therefore is capable of reducing DIM B to phthiotriol dimycocerosates. Since a focus on either DIM B or glycosylated phenolphthiodiolone dimycocerosates is sufficient to identify the electron source utilized in the reduction of the keto group of the phthiodiolone moiety, we limited the scope of our work to only the conversion of DIM B to DIM A (the nonglycosylated forms) in *M. bovis* BCG (52). We examined the DIM A and DIM B contents of wild-type *M. bovis* BCG strain Pasteur 1173P2 and a respective mutant strain (*fgd*::Tn*5367*) lacking functional *fgd* (BCG_0446 ORF) (25) via TLC

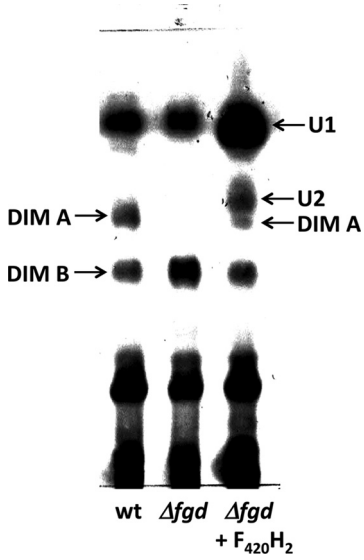

FIG 3 Analysis of dimycocerosates extracted from *Mycobacterium bovis* BCG strains and an *in vitro* conversion system via thin-layer chromatography (TLC). Lanes: wt, *M. bovis* BCG strain Pasteur 1173P2; Δ*fgd*, *M. bovis* BCG *fgd*::Tn*5367*; Δ*fgd* + $F_{420}H_2$, an *in vitro* reaction mixture containing a broken-cell suspension of *M. bovis* BCG *fgd*::Tn*5367* (source of DIM B and fPKR) and $F_{420}H_2$ generated *in situ* from F_{420} and glucose-6-phosphate by the action of a purified recombinant form of Fgd of *Mycobacterium smegmatis*. The details of the *in vitro* reaction, extraction of apolar lipids from mycobacterial cells and the *in vitro* reaction mixture, and TLC analysis of apolar lipids appear in Materials and Methods. The TLC analysis detected DIM A and DIM B but not the respective phenolic glycolipids. DIM A and DIM B bands are marked; the identities of U1 and U2 are unknown.

analysis. The resulting profile for *M. bovis* BCG *fgd*::Tn*5367* (Fig. 3, Δ*fgd* lane), which lacked $F_{420}H_2$ (the reductant), was similar to that observed previously with an *M. tuberculosis* H37Rv derivative lacking the Rv2951c protein (the reductase enzyme) (13). To validate the TLC data, we performed MALDI mass spectrometric analysis with the materials recovered from the specific bands. The DIM A and DIM B preparations obtained from the wild-type strain (Fig. 3, wt lane) yielded characteristic spectra (Fig. 4) (13, 53). The observed $[\text{DIM A} + \text{Na}]^+$ ion, with an *m/z* value of 1,348.738 (Fig. 4, left panel), represents a molecule with 89 carbon atoms (C_{89} species; theoretical mass, 1,348.3409) that has been reported for the highest-intensity peak in the mass spectrum for a DIM A preparation from *M. bovis* BCG strain Tokyo 172 (13, 54). The *m/z* values for other ions were higher or lower than that for the C_{89} species, by $n \times 14$ units (Fig. 4, left panel), and this result is consistent with *n* representing larger or smaller numbers of methylene (CH_2) groups present in the respective molecules. Similarly, the DIM B preparation produced an ion with an *m/z* value of 1,332.541 (Fig. 4, right panel), which is 16 mass units lower than that of the above-mentioned $[\text{DIM A} + \text{Na}]^+$ ion, with 89 carbon atoms (Fig. 4, left panel). This difference represents the conversion of a carbonyl group (C=O, as in DIM B) to a methoxy group (CH-OCH_3, as in DIM A). Several other peaks in the DIM B spectrum had cognate peaks in the DIM A spectrum (Fig. 4). A mass spectrometric analysis of DIM B isolated from the *fgd*::Tn*5367* strain (Fig. 3, Δ*fgd* lane) produced the same results (data not shown). These findings clearly establish that *M. bovis* BCG *fgd*::Tn*5367* lacks DIM A and accumulates DIM B. Since *M. bovis* BCG *fgd*::Tn*5367* carries a homolog of the Rv2951c protein or phthiodiolone ketoreductase (the BCG_2972c protein), the inability to convert DIM B to DIM A was due to the unavailability of $F_{420}H_2$, which prevented the generation of the phthiotriol intermediate, the methylation substrate (Fig. 1) (14, 15). An obvious explanation for this observation is that the BCG_2972c protein (a homolog of the Rv2951c protein of *M. tuberculosis*) is an $F_{420}H_2$-dependent phthiodiolone ketoreductase (fPKR).

Phthiodiolone ketoreductase reaction. The phthiodiolone ketoreductase reaction is as follows: phthiodiolone + $F_{420}H_2$ →

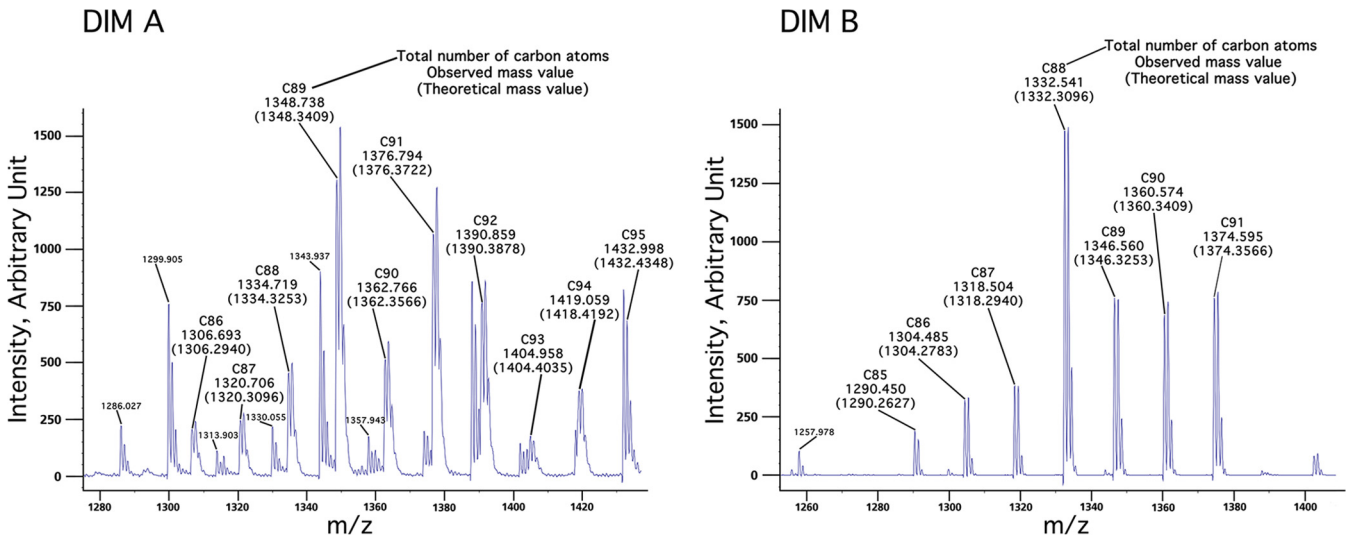

FIG 4 MALDI-TOF mass spectra of phthiodiolone dimycocerosates (DIM B) and phthiocerol dimycocerosates (DIM A) recovered from wild-type *Mycobacterium bovis* BCG (strain Pasteur 1173P2). The products analyzed correspond to the wt lane in Fig. 3. The peaks for $[\text{M} + \text{Na}]^+$ species with exclusively the ^{12}C isotope that are characteristic of DIM A and DIM B of *M. bovis* BCG (13) are labeled with their respective numbers of carbon atoms and observed *m/z* values. For each ion, the respective theoretical mass value (72) is shown within parentheses. The observed *m/z* values deviated from the theoretical mass values by 0.34 to 0.64 unit for $[\text{DIM A} + \text{Na}]^+$ ions and by 0.19 to 0.24 unit for $[\text{DIM B} + \text{Na}]^+$ ions. Such deviations have been observed by mass spectrometry analysis of DIM A and DIM B of *Mycobacterium bovis* BCG (54).

phthiotriol + F_{420}. Alternatively, $F_{420}H_2$ may serve as an indirect source of reductant for phthiodiolone reduction. Resolution of these possibilities would require demonstration of enzymatic and/or F_{420}-binding activity of the homogeneous enzyme.

Demonstration of $F_{420}H_2$-dependent phthiodiolone ketoreductase activity in cell extracts. We validated the conclusion derived from genetic analysis at the enzymatic activity level. In this experiment, a broken-cell slurry of *M. bovis* BCG *fgd*::Tn*5367* was used as the source of phthiodiolone dimycocerosate (DIM B) and phthiodiolone reductase (the BCG_2972c protein), and the needed $F_{420}H_2$ was generated *in situ* from added F_{420}, glucose-6-phosphate, and purified Fgd via the following reaction: glucose-6-phosphate + $F_{420} \rightarrow F_{420}H_2$ + 6-phosphogluconate. A TLC analysis showed that upon incubation at 37°C, the system converted DIM B present in *M. bovis* BCG *fgd*::Tn*5367* to a DIM A-like product and two other compounds that were assigned the trivial names U1 and U2 (Fig. 3, Δ*fgd* + $F_{420}H_2$ lane). The putative DIM A product isolated from the *in vitro* reaction mixture was analyzed via MALDI mass spectrometry, and in the resulting spectrum the following peaks had *m/z* values (numbers of carbon atoms) characteristic of DIM A: 1,348.354 (C_{89}), 1,362.179 (C_{90}), 1,376.245 (C_{91}), 1,390.249 (C_{92}), 1,404.360 (C_{93}), 1,418.424 (C_{94}), 1,432.277 (C_{95}), and 1,446.239 (C_{96}). The other reaction products, U1 and U2 (Fig. 3, Δ*fgd* + $F_{420}H_2$ lane), remain to be identified, but the former seemed to exist in wild-type *M. bovis* BCG (Fig. 3, wt lane). These results showed that the *in vitro* reaction that was catalyzed by the enzyme systems from the mutant strain (*fgd*::Tn*5367*) and utilized $F_{420}H_2$ generated by purified Fgd as a reductant converted DIM B to DIM A. This conversion must have occurred in two steps: $F_{420}H_2$-dependent reduction of DIM B to the respective phthiotriol derivatives, catalyzed by the BCG_2972c protein; and methylation of phthiotriols to phthiocerols (DIM A) by a methyltransferase, the BCG_2973 protein. It remains to be investigated whether the production of U1 or U2 was caused by Fgd, $F_{420}H_2$, glucose-6-phosphate, 6-phosphogluconate, fPKR, or other enzymes of *M. bovis* BCG.

Phylogenetic analysis of mycobacterial homologs of the Rv2951c protein (fPKR), revealing potentially new F_{420}-dependent lipid-modifying enzymes in mycobacteria. The homologs of the full-length Rv2951c protein identified in the BLASTP search fell into two distinct groups in terms of amino acid sequence identity with the Rv2951c protein: those with ≥50% and those with ≤40% identity. This selection was justified by the absence of homologs in the intermediate range and therefore provided a sharp boundary. The ≤40% group included F_{420}-dependent glucose-6-phosphate dehydrogenase (Fgd) (18, 19), F_{420}-dependent hydroxymycolic acid dehydrogenase (fHMAD) (39), and putative flavin-containing enzymes. On the other hand, the ≥50% group was comprised of phthiodiolone ketoreductases and proteins of unknown function, and due to this closer relationship with the Rv2951c protein, we performed a maximum likelihood-based phylogenetic analysis with select representatives of this group (Fig. 5); the full-length sequence of every homolog, with appropriate trimming as described in Materials and Methods, was used in the analysis. The analysis revealed major clades, each of which had two or more subgroups (Fig. 5). Clade Ia represented the closest homologs of fPKR (with >83% amino acid sequence identities with the Rv2951c protein). These proteins belonged to a group of slow-growing mycobacteria which are known to contain PDIM (55) and to carry PapA5, which catalyzes a committed step of PDIM synthesis in *M. tuberculosis* (56). PapA5, a polyketide-associated protein, is an acyltransferase, and the respective gene is part of a PDIM synthesis gene cluster (7–9, 14, 50, 57–59). Accordingly, clade Ia homologs of the Rv2951c protein are likely to be *bona fide* fPKRs. Also, with the exception of *Mycobacterium gastri*, all species carrying clade Ia homologs are human or animal pathogens (55) (Fig. 5). This pattern is consistent with the observation that PDIM is one of the pathogenicity determinants of mycobacteria (3–11). Clade Ib homologs and most members of clade II were from fast-growing mycobacterial species (Fig. 5), and the available data suggest that these organisms are devoid of PDIM (55). A BLASTP analysis showed that these species harbored weaker homologs of PapA5 that exhibited 40% amino acid sequence identity to *M. tuberculosis* PapA5; for the organisms with PDIM, the respective sequence identity values were >80%. However, every protein shown in Fig. 5 carried the conserved F_{420}-binding residues shown in Fig. 2 (data not shown). Accordingly, we hypothesize that clade Ib and II homologs reduce keto groups or oxidize hydroxyl groups on lipids or lipid domains of more complex compounds by using F_{420} as an electron carrier.

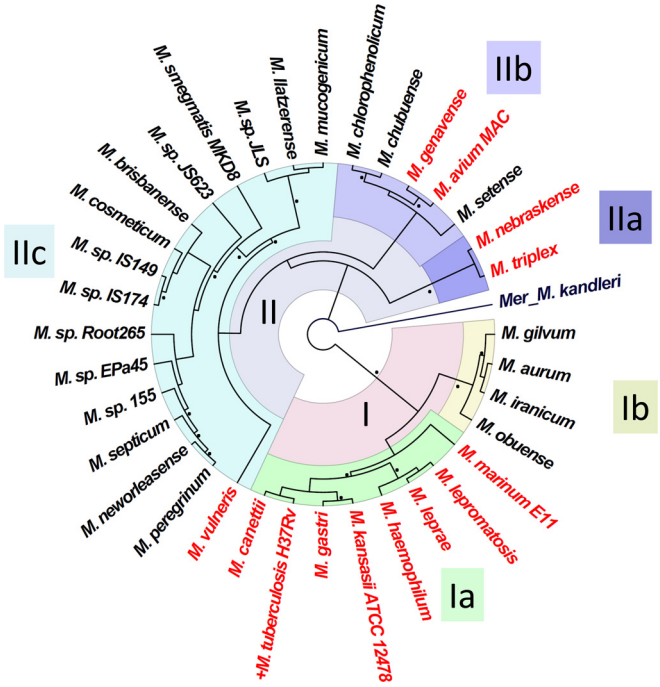

FIG 5 Maximum likelihood phylogenetic analysis of $F_{420}H_2$-dependent phthiodiolone ketoreductase (fPKR) homologs in mycobacteria. Homologs with amino acid sequence identities to *Mycobacterium tuberculosis* fPKR (the Rv2915c protein) of >50% were analyzed, and the method was performed as described previously (32). The coenzyme F_{420}-dependent N^5,N^{10}-methylene tetrahydromethanopterin reductase (Mer) from *Methanopyrus kandleri* (37) was used as the outgroup. The names of the slow-growing mycobacterial species (52) and the respective Rv2951c protein homologs are shown in red; the rest are fast growers (52). +, the fPKRs of *M. tuberculosis* H37Rv (the Rv2951c protein) and *M. bovis* BCG strain Pasteur 1173P2 (the BCG_2972c protein) have identical amino acid sequences. The dots near the branches indicate bootstrap values of >70 (calculated for 100 replicates). The homologs in clade Ia are >80% identical to the Rv2951c protein at the amino acid sequence level and belong to slow-growing mycobacterial species that contain PDIM (52, 55) and carry the gene for an acyltransferase (PapA5) that catalyzes the committed step of PDIM biosynthesis (56). With the exception of *Mycobacterium gastri*, the species harboring clade Ia homologs are human or animal pathogens (55).

fPKR expands the list of experimentally validated F_{420}-dependent enzymes in *M. tuberculosis* to six (18, 39, 60), among which Fgd, fHMAD, and fPKR are Mer homologs (Fig. 2) (18, 19, 39) and the others are $F_{420}H_2$-dependent quinone reductases (Fqr) or Ddn family proteins (the Rv3547, Rv1261c, and Rv1558 proteins) (60). These enzymes represent a part of the full potential, as *M. tuberculosis* has been predicted to carry at least 28 F_{420}-dependent enzymes (20), and one of the identified Ddn homologs (the Rv3178 protein) has yet to be studied for enzymatic activity (60). This is an important gap, as all F_{420}-dependent systems of *M. tuberculosis* investigated thus far have been linked to TB pathogenesis and/or found to be relevant to the development of TB therapeutics (26, 39, 60, 61). Fgd is the principal enzyme for the generation of reduced $F_{420}H_2$ (18, 44, 49), which is likely used by *M. tuberculosis* in combating oxidative or nitrosative stress (44, 49, 60). For example, $F_{420}H_2$ allows this pathogen to covert highly toxic nitrogen dioxide (NO_2) to nitric oxide (NO) via chemical reduction (44); the organism is very sensitive to NO_2 and almost resistant to NO (44, 62). Similarly, a mutant strain of *M. tuberculosis* that is devoid of F_{420} is hypersensitive to oxidative stress, as it cannot provide $F_{420}H_2$ for the three $F_{420}H_2$-dependent quinone reductases discussed above, which protect mycobacteria against oxidative stress (60). One of these reductases (Ddn, encoded by the Rv3547 ORF) acts as a nitroreductase to activate a prodrug called PA-824, a promising anti-TB drug that acts in concert with $F_{420}H_2$ (45, 60, 63, 64). The hydroxymycolic acid dehydrogenase (fHMAD), which generates ketomycolic acids (K-MA) from hydroxymycolic acids (H-MA), and fPKR studied here exemplify the critical role of F_{420} in the functionalization of the formidable cell wall lipids that protect *M. tuberculosis* from the host immune attack and from anti-TB drugs (12, 39, 61, 65–70). Also, fHMAD is one of the targets of PA-824 (39). Some of the mycobacterial F_{420}-dependent enzymes catalyze decolorization of triphenylmethane dyes and degradation of aflatoxins (22, 46, 48, 71), and it is likely that these enzymes catalyze more physiologically relevant cellular functions *in vivo*, some of which may have roles in TB pathogenesis. The information presented in Fig. 5 brings several potentially novel F_{420}-dependent lipid-modifying enzymes into focus. Thus, this report, in addition to defining the electron donor requirement of an important enzyme of pathogenic mycobacteria, further emphasizes a broad influence of F_{420} in the physiology of the mycobacteria in general.

ACKNOWLEDGMENTS

We thank Su Jung Kang for assistance with the purification of recombinant F_{420}-dependent glucose-6-phosphate dehydrogenase, Dwi Susanti for consultation on phylogenetic analysis, and Furong Sun and Kevin R. Tucker, Mass Spectrometry Lab, School of Chemical Sciences, University of Illinois at Urbana-Champaign, for their help with mass spectrometry.

This research was supported by grant 1R21AI100039 from the National Institutes of Health. B.M. was supported in part by the Virginia Tech and Agricultural Experiment Station Hatch Program (CRIS project VA-160021).

FUNDING INFORMATION

This work, including the efforts of Endang Purwantini and Biswarup Mukhopadhyay, was funded by HHS | National Institutes of Health (NIH) (1R21AI100039).

REFERENCES

1. **Daffe M, Lacave C, Laneelle MA, Laneelle G.** 1987. Structure of the major triglycosyl phenol-phthiocerol of *Mycobacterium tuberculosis* (strain Canetti). Eur J Biochem **167:**155–160. http://dx.doi.org/10.1111/j.1432-1033.1987.tb13317.x.
2. **Daffe M, Laneelle MA.** 1989. Diglycosyl phenol phthiocerol diester of *Mycobacterium leprae*. Biochim Biophys Acta **1002:**333–337. http://dx.doi.org/10.1016/0005-2760(89)90347-0.
3. **Jain M, Petzold CJ, Schelle MW, Leavell MD, Mougous JD, Bertozzi CR, Leary JA, Cox JS.** 2007. Lipidomics reveals control of *Mycobacterium tuberculosis* virulence lipids via metabolic coupling. Proc Natl Acad Sci U S A **104:**5133–5138. http://dx.doi.org/10.1073/pnas.0610634104.
4. **Guenin-Mace L, Simeone R, Demangel C.** 2009. Lipids of pathogenic mycobacteria: contributions to virulence and host immune suppression. Transbound Emerg Dis **56:**255–268. http://dx.doi.org/10.1111/j.1865-1682.2009.01072.x.
5. **Minnikin DE, Dobson G, Draper P.** 1985. The free lipids of *Mycobacterium leprae* harvested from experimentally infected nine-banded armadillos. J Gen Microbiol **131:**2007–2011.
6. **Ng V, Zanazzi G, Timpl R, Talts JF, Salzer JL, Brennan PJ, Rambukkana A.** 2000. Role of the cell wall phenolic glycolipid-1 in the peripheral nerve predilection of *Mycobacterium leprae*. Cell **103:**511–524. http://dx.doi.org/10.1016/S0092-8674(00)00142-2.
7. **Reed MB, Domenech P, Manca C, Su H, Barczak AK, Kreiswirth BN, Kaplan G, Barry CE, III.** 2004. A glycolipid of hypervirulent tuberculosis strains that inhibits the innate immune response. Nature **431:**84–87. http://dx.doi.org/10.1038/nature02837.
8. **Camacho LR, Ensergueix D, Perez E, Gicquel B, Guilhot C.** 1999. Identification of a virulence gene cluster of *Mycobacterium tuberculosis* by signature-tagged transposon mutagenesis. Mol Microbiol **34:**257–267. http://dx.doi.org/10.1046/j.1365-2958.1999.01593.x.
9. **Cox JS, Chen B, McNeil M, Jacobs WR, Jr.** 1999. Complex lipid determines tissue-specific replication of *Mycobacterium tuberculosis* in mice. Nature **402:**79–83. http://dx.doi.org/10.1038/47042.
10. **Rousseau C, Winter N, Pivert E, Bordat Y, Neyrolles O, Ave P, Huerre M, Gicquel B, Jackson M.** 2004. Production of phthiocerol dimycocerosates protects *Mycobacterium tuberculosis* from the cidal activity of reactive nitrogen intermediates produced by macrophages and modulates the early immune response to infection. Cell Microbiol **6:**277–287. http://dx.doi.org/10.1046/j.1462-5822.2004.00368.x.
11. **Sirakova TD, Dubey VS, Kim HJ, Cynamon MH, Kolattukudy PE.** 2003. The largest open reading frame (pks12) in the *Mycobacterium tuberculosis* genome is involved in pathogenesis and dimycocerosyl phthiocerol synthesis. Infect Immun **71:**3794–3801. http://dx.doi.org/10.1128/IAI.71.7.3794-3801.2003.
12. **Day TA, Mittler JE, Nixon MR, Thompson C, Miner MD, Hickey MJ, Liao RP, Pang JM, Shayakhmetov DM, Sherman DR.** 2014. *Mycobacterium tuberculosis* strains lacking surface lipid phthiocerol dimycocerosate are susceptible to killing by an early innate host response. Infect Immun **82:**5214–5222. http://dx.doi.org/10.1128/IAI.01340-13.
13. **Simeone R, Constant P, Malaga W, Guilhot C, Daffe M, Chalut C.** 2007. Molecular dissection of the biosynthetic relationship between phthiocerol and phthiodiolone dimycocerosates and their critical role in the virulence and permeability of *Mycobacterium tuberculosis*. FEBS J **274:**1957–1969. http://dx.doi.org/10.1111/j.1742-4658.2007.05740.x.
14. **Onwueme KC, Vos CJ, Zurita J, Soll CE, Quadri LE.** 2005. Identification of phthiodiolone ketoreductase, an enzyme required for production of mycobacterial diacyl phthiocerol virulence factors. J Bacteriol **187:**4760–4766. http://dx.doi.org/10.1128/JB.187.14.4760-4766.2005.
15. **Perez E, Constant P, Laval F, Lemassu A, Laneelle MA, Daffe M, Guilhot C.** 2004. Molecular dissection of the role of two methyltransferases in the biosynthesis of phenolglycolipids and phthiocerol dimycoserosate in the *Mycobacterium tuberculosis* complex. J Biol Chem **279:**42584–42592. http://dx.doi.org/10.1074/jbc.M406134200.
16. **DiMarco AA, Bobik TA, Wolfe RS.** 1990. Unusual coenzymes of methanogenesis. Annu Rev Biochem **59:**355–394. http://dx.doi.org/10.1146/annurev.bi.59.070190.002035.
17. **Bashiri G, Squire CJ, Moreland NJ, Baker EN.** 2008. Crystal structures of F_{420}-dependent glucose-6-phosphate dehydrogenase FGD1 involved in the activation of the anti-tuberculosis drug candidate PA-824 reveal the basis of coenzyme and substrate binding. J Biol Chem **283:**17531–17541. http://dx.doi.org/10.1074/jbc.M801854200.
18. **Purwantini E, Daniels L.** 1996. Purification of a novel coenzyme F_{420}-dependent glucose-6-phosphate dehydrogenase from *Mycobacterium smegmatis*. J Bacteriol **178:**2861–2866.
19. **Purwantini E, Daniels L.** 1998. Molecular analysis of the gene encoding

F_{420}-dependent glucose-6-phosphate dehydrogenase from *Mycobacterium smegmatis*. J Bacteriol **180:**2212–2219.

20. **Selengut JD, Haft DH.** 2010. Unexpected abundance of coenzyme F_{420}-dependent enzymes in *Mycobacterium tuberculosis* and other actinobacteria. J Bacteriol **192:**5788–5798. http://dx.doi.org/10.1128/JB.00425-10.
21. **Daniels L, Bakhiet N, Harmon K.** 1985. Widespread distribution of a 5-deazaflavin cofactor in *Actinomyces* and related bacteria. Syst Appl Microbiol **6:**12–17. http://dx.doi.org/10.1016/S0723-2020(85)80004-7.
22. **Graham DE.** 2010. A new role for coenzyme F_{420} in aflatoxin reduction by soil mycobacteria. Mol Microbiol **78:**533–536. http://dx.doi.org/10.1111/j.1365-2958.2010.07358.x.
23. **Purwantini E, Gillis TP, Daniels L.** 1997. Presence of F_{420}-dependent glucose-6-phosphate dehydrogenase in *Mycobacterium* and *Nocardia* species, but absence from *Streptomyces* and *Corynebacterium* species and methanogenic archaea. FEMS Microbiol Lett **146:**129–134. http://dx.doi.org/10.1111/j.1574-6968.1997.tb10182.x.
24. **Walsh CT.** 1986. Naturally occurring 5-deazaflavin coenzymes: biological redox roles. Acc Chem Res **19:**216–221. http://dx.doi.org/10.1021/ar00127a004.
25. **Brosch R, Gordon SV, Garnier T, Eiglmeier K, Frigui W, Valenti P, Dos Santos S, Duthoy S, Lacroix C, Garcia-Pelayo C, Inwald JK, Golby P, Garcia JN, Hewinson RG, Behr MA, Quail MA, Churcher C, Barrell BG, Parkhill J, Cole ST.** 2007. Genome plasticity of BCG and impact on vaccine efficacy. Proc Natl Acad Sci U S A **104:**5596–5601. http://dx.doi.org/10.1073/pnas.0700869104.
26. **Choi KP, Bair TB, Bae YM, Daniels L.** 2001. Use of transposon Tn5367 mutagenesis and a nitroimidazopyran-based selection system to demonstrate a requirement for *fbiA* and *fbiB* in coenzyme F(420) biosynthesis by *Mycobacterium bovis* BCG. J Bacteriol **183:**7058–7066. http://dx.doi.org/10.1128/JB.183.24.7058-7066.2001.
27. **Parish T, Stoker NG (ed).** 2001. *Mycobacterium tuberculosis* protocols. Humana Press, Totowa, NJ.
28. **Rocco CJ, Dennison KL, Klenchin VA, Rayment I, Escalante-Semerena JC.** 2008. Construction and use of new cloning vectors for the rapid isolation of recombinant proteins from *Escherichia coli*. Plasmid **59:**231–237. http://dx.doi.org/10.1016/j.plasmid.2008.01.001.
29. **Case CL, Concar EM, Boswell KL, Mukhopadhyay B.** 2006. Roles of Asp^{75}, Asp^{78}, and Glu^{83} of GTP-dependent phosphoenolpyruvate carboxykinase from *Mycobacterium smegmatis*. J Biol Chem **281:**39262–39272. http://dx.doi.org/10.1074/jbc.M602591200.
30. **Lai H, Kraszewski JL, Purwantini E, Mukhopadhyay B.** 2006. Identification of pyruvate carboxylase genes in *Pseudomonas aeruginosa* PAO1 and development of a *P. aeruginosa*-based overexpression system for alpha4- and alpha4beta4-type pyruvate carboxylases. Appl Environ Microbiol **72:**7785–7792. http://dx.doi.org/10.1128/AEM.01564-06.
31. **Altschul S, Madden T, Schaffer A, Zhang J, Zhang Z, Miller W, Lipman D.** 1997. Gapped BLAST and PSI-BLAST: a new generation of protein database search programs. Nucleic Acids Res **25:**3389–3402. http://dx.doi.org/10.1093/nar/25.17.3389.
32. **Susanti D, Mukhopadhyay B.** 2012. An intertwined evolutionary history of methanogenic archaea and sulfate reduction. PLoS One **7:**e45313. http://dx.doi.org/10.1371/journal.pone.0045313.
33. **Edgar RC.** 2004. MUSCLE: multiple sequence alignment with high accuracy and high throughput. Nucleic Acids Res **32:**1792–1797. http://dx.doi.org/10.1093/nar/gkh340.
34. **Castresana J.** 2000. Selection of conserved blocks from multiple alignments for their use in phylogenetic analysis. Mol Biol Evol **17:**540–552. http://dx.doi.org/10.1093/oxfordjournals.molbev.a026334.
35. **Aufhammer SW, Warkentin E, Berk H, Shima S, Thauer RK, Ermler U.** 2004. Coenzyme binding in F_{420}-dependent secondary alcohol dehydrogenase, a member of the bacterial luciferase family. Structure **12:**361–370. http://dx.doi.org/10.1016/j.str.2004.02.010.
36. **Aufhammer SW, Warkentin E, Ermler U, Hagemeier CH, Thauer RK, Shima S.** 2005. Crystal structure of methylenetetrahydromethanopterin reductase (Mer) in complex with coenzyme F_{420}: architecture of the F_{420}/FMN binding site of enzymes within the nonprolyl *cis*-peptide containing bacterial luciferase family. Protein Sci **14:**1840–1849. http://dx.doi.org/10.1110/ps.041289805.
37. **Shima S, Warkentin E, Grabarse W, Sordel M, Wicke M, Thauer RK, Ermler U.** 2000. Structure of coenzyme F_{420}-dependent methylenetetrahydromethanopterin reductase from two methanogenic archaea. J Mol Biol **300:**935–950. http://dx.doi.org/10.1006/jmbi.2000.3909.
38. **Pei J, Kim BH, Grishin NV.** 2008. PROMALS3D: a tool for multiple protein sequence and structure alignments. Nucleic Acids Res **36:**2295–2300. http://dx.doi.org/10.1093/nar/gkn072.
39. **Purwantini E, Mukhopadhyay B.** 2013. Rv0132c of *Mycobacterium tuberculosis* encodes a coenzyme F_{420}-dependent hydroxymycolic acid dehydrogenase. PLoS One **8:**e81985. http://dx.doi.org/10.1371/journal.pone.0081985.
40. **Biro JC.** 2006. Amino acid size, charge, hydropathy indices and matrices for protein structure analysis. Theor Biol Med Model **3:**15. http://dx.doi.org/10.1186/1742-4682-3-15.
41. **Chothia C.** 1976. The nature of the accessible and buried surfaces in proteins. J Mol Biol **105:**1–12. http://dx.doi.org/10.1016/0022-2836(76)90191-1.
42. **Creighton TE.** 1993. Proteins: structures and molecular properties. W H Freeman & Co, New York, NY.
43. **Zamyatnin AA.** 1972. Protein volume in solution. Prog Biophys Mol Biol **24:**107–123. http://dx.doi.org/10.1016/0079-6107(72)90005-3.
44. **Purwantini E, Mukhopadhyay B.** 2009. Conversion of NO_2 to NO by reduced coenzyme F_{420} protects mycobacteria from nitrosative damage. Proc Natl Acad Sci U S A **106:**6333–6338. http://dx.doi.org/10.1073/pnas.0812883106.
45. **Stover CK, Warrener P, VanDevanter DR, Sherman DR, Arain TM, Langhorne MH, Anderson SW, Towell JA, Yuan Y, McMurray DN, Kreiswirth BN, Barry CE, Baker WR.** 2000. A small-molecule nitroimidazopyran drug candidate for the treatment of tuberculosis. Nature **405:**962–966. http://dx.doi.org/10.1038/35016103.
46. **Manjunatha U, Boshoff HI, Barry CE.** 2009. The mechanism of action of PA-824: novel insights from transcriptional profiling. Commun Integr Biol **2:**215–218. http://dx.doi.org/10.4161/cib.2.3.7926.
47. **Manjunatha UH, Boshoff H, Dowd CS, Zhang L, Albert TJ, Norton JE, Daniels L, Dick T, Pang SS, Barry CE, III.** 2006. Identification of a nitroimidazo-oxazine-specific protein involved in PA-824 resistance in *Mycobacterium tuberculosis*. Proc Natl Acad Sci U S A **103:**431–436. http://dx.doi.org/10.1073/pnas.0508392103.
48. **Taylor MC, Jackson CJ, Tattersall DB, French N, Peat TS, Newman J, Briggs LJ, Lapalikar GV, Campbell PM, Scott C, Russell RJ, Oakeshott JG.** 2010. Identification and characterization of two families of $F_{420}H_2$-dependent reductases from mycobacteria that catalyse aflatoxin degradation. Mol Microbiol **78:**561–575. http://dx.doi.org/10.1111/j.1365-2958.2010.07356.x.
49. **Hasan MR, Rahman M, Jaques S, Purwantini E, Daniels L.** 2010. Glucose 6-phosphate accumulation in mycobacteria: implications for a novel F_{420}-dependent anti-oxidant defense system. J Biol Chem **285:**19135–19144. http://dx.doi.org/10.1074/jbc.M109.074310.
50. **Azad AK, Sirakova TD, Rogers LM, Kolattukudy PE.** 1996. Targeted replacement of the mycocerosic acid synthase gene in *Mycobacterium bovis* BCG produces a mutant that lacks mycosides. Proc Natl Acad Sci U S A **93:**4787–4792. http://dx.doi.org/10.1073/pnas.93.10.4787.
51. **Ferreras JA, Stirrett KL, Lu X, Ryu JS, Soll CE, Tan DS, Quadri LE.** 2008. Mycobacterial phenolic glycolipid virulence factor biosynthesis: mechanism and small-molecule inhibition of polyketide chain initiation. Chem Biol **15:**51–61. http://dx.doi.org/10.1016/j.chembiol.2007.11.010.
52. **Rastogi N, Legrand E, Sola C.** 2001. The mycobacteria: an introduction to nomenclature and pathogenesis. Rev Sci Tech **20:**21–54.
53. **Daffe M, Laneelle MA.** 1988. Distribution of phthiocerol diester, phenolic mycosides and related compounds in mycobacteria. J Gen Microbiol **134:**2049–2055.
54. **Naka T, Maeda S, Niki M, Ohara N, Yamamoto S, Yano I, Maeyama J, Ogura H, Kobayashi K, Fujiwara N.** 2011. Lipid phenotype of two distinct subpopulations of *Mycobacterium bovis* bacillus Calmette-Guerin Tokyo 172 substrain. J Biol Chem **286:**44153–44161. http://dx.doi.org/10.1074/jbc.M111.310037.
55. **Onwueme KC, Vos CJ, Zurita J, Ferreras JA, Quadri LE.** 2005. The dimycocerosate ester polyketide virulence factors of mycobacteria. Prog Lipid Res **44:**259–302. http://dx.doi.org/10.1016/j.plipres.2005.07.001.
56. **Chavadi SS, Onwueme KC, Edupuganti UR, Jerome J, Chatterjee D, Soll CE, Quadri LE.** 2012. The mycobacterial acyltransferase PapA5 is required for biosynthesis of cell wall-associated phenolic glycolipids. Microbiology **158:**1379–1387. http://dx.doi.org/10.1099/mic.0.057869-0.
57. **Azad AK, Sirakova TD, Fernandes ND, Kolattukudy PE.** 1997. Gene knockout reveals a novel gene cluster for the synthesis of a class of cell wall lipids unique to pathogenic mycobacteria. J Biol Chem **272:**16741–16745. http://dx.doi.org/10.1074/jbc.272.27.16741.
58. **Quadri LE, Sello J, Keating TA, Weinreb PH, Walsh CT.** 1998. Identification of a *Mycobacterium tuberculosis* gene cluster encoding the

biosynthetic enzymes for assembly of the virulence-conferring siderophore mycobactin. Chem Biol **5:**631–645. http://dx.doi.org/10.1016/S1074-5521(98)90291-5.

59. **Yu J, Tran V, Li M, Huang X, Niu C, Wang D, Zhu J, Wang J, Gao Q, Liu J.** 2012. Both phthiocerol dimycocerosates and phenolic glycolipids are required for virulence of Mycobacterium marinum. Infect Immun **80:**1381–1389. http://dx.doi.org/10.1128/IAI.06370-11.
60. **Gurumurthy M, Rao M, Mukherjee T, Rao SP, Boshoff HI, Dick T, Barry CE, III, Manjunatha UH.** 2013. A novel F(420)-dependent antioxidant mechanism protects *Mycobacterium tuberculosis* against oxidative stress and bactericidal agents. Mol Microbiol **87:**744–755. http://dx.doi.org/10.1111/mmi.12127.
61. **Dao DN, Sweeney K, Hsu T, Gurcha SS, Nascimento IP, Roshevsky D, Besra GS, Chan J, Porcelli SA, Jacobs WR.** 2008. Mycolic acid modification by the *mmaA4* gene of *M. tuberculosis* modulates IL-12 production. PLoS Pathog **4:**e1000081. http://dx.doi.org/10.1371/journal.ppat.1000081.
62. **Yu K, Mitchell C, Xing Y, Magliozzo RS, Bloom BR, Chan J.** 1999. Toxicity of nitrogen oxides and related oxidants on mycobacteria: *M. tuberculosis* is resistant to peroxynitrite anion. Tuber Lung Dis **79:**191–198. http://dx.doi.org/10.1054/tuld.1998.0203.
63. **Matsumoto M, Hashizume H, Tomishige T, Kawasaki M, Tsubouchi H, Sasaki H, Shimokawa Y, Komatsu M.** 2006. OPC-67683, a nitro-dihydro-imidazooxazole derivative with promising action against tuberculosis in vitro and in mice. PLoS Med **3:**e466. http://dx.doi.org/10.1371/journal.pmed.0030466.
64. **Singh R, Manjunatha U, Boshoff HI, Ha YH, Niyomrattanakit P, Ledwidge R, Dowd CS, Lee IY, Kim P, Zhang L, Kang S, Keller TH, Jiricek J, Barry CE, III.** 2008. PA-824 kills nonreplicating *Mycobacterium tuberculosis* by intracellular NO release. Science **322:**1392–1395. http://dx.doi.org/10.1126/science.1164571.
65. **Sambandan D, Dao DN, Weinrick BC, Vilcheze C, Gurcha SS, Ojha A, Kremer L, Besra GS, Hatfull GF, Jacobs WR, Jr.** 2013. Keto-mycolic acid-dependent pellicle formation confers tolerance to drug-sensitive *Mycobacterium tuberculosis*. mBio **4:**e00222-13. http://dx.doi.org/10.1128/mBio.00222-13.
66. **Dubnau E, Chan J, Raynaud C, Mohan VP, Laneelle MA, Yu K, Quemard A, Smith I, Daffe M.** 2000. Oxygenated mycolic acids are necessary for virulence of *Mycobacterium tuberculosis* in mice. Mol Microbiol **36:**630–637.
67. **Yuan Y, Zhu Y, Crane DD, Barry CE, III.** 1998. The effect of oxygenated mycolic acid composition on cell wall function and macrophage growth in *Mycobacterium tuberculosis*. Mol Microbiol **29:**1449–1458. http://dx.doi.org/10.1046/j.1365-2958.1998.01026.x.
68. **Vander Beken S, Al Dulayymi JR, Naessens T, Koza G, Maza-Iglesias M, Rowles R, Theunissen C, De Medts J, Lanckacker E, Baird MS, Grooten J.** 2011. Molecular structure of the *Mycobacterium tuberculosis* virulence factor, mycolic acid, determines the elicited inflammatory pattern. Eur J Immunol **41:**450–460. http://dx.doi.org/10.1002/eji.201040719.
69. **Beukes M, Lemmer Y, Deysel M, Al Dulayymi JR, Baird MS, Koza G, Iglesias MM, Rowles RR, Theunissen C, Grooten J, Toschi G, Roberts VV, Pilcher L, Van Wyngaardt S, Mathebula N, Balogun M, Stoltz AC, Verschoor JA.** 2010. Structure-function relationships of the antigenicity of mycolic acids in tuberculosis patients. Chem Phys Lipids **163:**800–808. http://dx.doi.org/10.1016/j.chemphyslip.2010.09.006.
70. **Rao V, Gao F, Chen B, Jacobs WR, Glickman MS.** 2006. Trans-cyclopropanation of mycolic acids on trehalose dimycolate suppresses *Mycobacterium tuberculosis*-induced inflammation and virulence. J Clin Invest **116:**1660–1667. http://dx.doi.org/10.1172/JCI27335.
71. **Guerra-Lopez D, Daniels L, Rawat M.** 2007. *Mycobacterium smegmatis* mc^2 155 *fbiC* and MSMEG_2392 are involved in triphenylmethane dye decolorization and coenzyme F_{420} biosynthesis. Microbiology **153:**2724–2732. http://dx.doi.org/10.1099/mic.0.2006/009241-0.
72. **Layre E, Sweet L, Hong S, Madigan CA, Desjardins D, Young DC, Cheng TY, Annand JW, Kim K, Shamputa IC, McConnell MJ, Debono CA, Behar SM, Minnaard AJ, Murray M, Barry CE, III, Matsunaga I, Moody DB.** 2011. A comparative lipidomics platform for chemotaxonomic analysis of Mycobacterium tuberculosis. Chem Biol **18:**1537–1549. http://dx.doi.org/10.1016/j.chembiol.2011.10.013.